

Dissipation induced by attractive interaction in dynamic force microscopy : contribution of adsorbed water layers.

L. Nony^{1,*}, T. Cohen-Bouhacina², J.-P. Aimé²

¹ L2MP, UMR CNRS 6137, Université d'Aix-Marseille III

Faculté des Sciences de Saint-Jérôme, 13397 Marseille Cedex 20, FRANCE

² CPMOH, UMR CNRS 5798, Université Bordeaux I

351, cours de la Libération, 33405 Talence Cedex, FRANCE

* To whom correspondence should be addressed; E-mail: laurent.nony@l2mp.fr

published in *Surface Science* **499**, pp152-160 (2002)

Abstract

At room temperature and under ambient conditions, due to the adsorption, a water film is always present on silica surfaces. If the surface is investigated with a scanning probe method in Contact mode, this causes the formation of a meniscus between the tip and the surface. This liquid neck generates additional capillary forces between the nano-tip and the surface. In dynamic mode, due to the action of the oscillating tip on the surface, the mechanical response of the adsorbed water layers can induce additional dissipation that is probed through the phase variations of the oscillator. In the present work, we analyze by dynamic force microscopy the growth of a water film on a silica surface as a function of time. The silica sample is first cleaned and heated at 420°C, then is exposed to dry conditions. The influence of the water film is checked with the dynamic mode by using intermittent contact and noncontact situations. To describe the experimental observations, additional dissipation is taken into account when the tip approaches the surface. The results of the fits allow the evaluation of the dissipation induced by the attractive interaction between the tip and the silica surface related to the adsorption of water molecules on surface as a function of time. Results are compared to previous tribological studies performed in Contact mode and infra-red spectroscopy measurements on the silica for which the key parameter was the surface temperature instead of time. The two experimental results are in good agreement.

keywords : Atomic Force Microscopy, Adsorption kinetics, Growth, Silicon oxides.

PACS 05.45.-a, 07.79.Lh, 45.20.Jj

I. INTRODUCTION

During the last decade, Dynamic Force Microscopy (DFM) used in the Tapping mode has been found as a suitable tool to investigate surfaces morphology and mechanical properties of soft materials. The technics has been widely used to investigate a wide range of samples including polymers^{1,2}, biological materials^{3,4} or organic layers^{5,6}. Taking advantage of the sensitivity of the oscillating tip-cantilever system (OTCL) at the proximity of the surface, various physical properties can be investigated including mechanical properties^{7,8,9,10}, adhesion¹¹, forces mapping^{12,13,14} and dissipation processes^{15,16,17,18,19,20}. As a complementary approach, experiments performed in Contact mode were widely used to probe chemical treatments of surfaces and evolution of surface properties. Therefore, numerous works were dedicated to investigate adhesion and friction variations as a function of changes of the surface properties under various conditions : humidity rate, vacuum or controlled atmosphere^{21,22,23}.

Because DFM is a very sensitive tool probing forces is noncontact and intermittent contact situations, it is a suitable approach to investigate local properties without inducing severe damage on the surface. In particular, liquid layers and the influence of capillary forces have been extensively investigated^{24,25}. The presence of a liquid layer from molecular thickness up to a few nanometers can significantly modify the behavior of the OTCL. In ref.²⁵, M.Luna et al. discuss the influence of the conservative and non conservative forces due to the water adsorption onto various surfaces on the variation of the resonance frequency and quality factor of the OTCL.

In the present work, we use DFM to investigate the growth of a water film on a silica surface at room temperature as a function of the exposure time. To do so, we use recent theoretical developments describing the influence of the noncontact dissipation (NC dissipation) on the observed phase delay during a Tapping experiment^{20,26,27,28,29}. The silica surface is first cleaned and heated under oxygen flow at 420 °C during 90 minutes. Then, it is put into a glove box under controlled atmosphere assuming that the water covering goes along. Evolution of the surface is measured by recording approach-retract curves versus time that give the variations of the oscillation amplitude and phase as a function of the tip-surface distance.

In the first part of the paper, we briefly recall the model used to take into account the surface modifications and NC dissipation processes. The second part is devoted to

experimental results obtained with the cleaned and heated silica surface and a comparison with the theoretical developments. The experimental results are compared to those obtained with a previous tribological study performed in Contact mode as a function of the sample temperature. The last part of the paper is a discussion of the results obtained.

II. MODELING THE OTCL'S BEHAVIOR

The present section gives a synthesis of the theoretical developments allowing analytical expressions of the nonlinear equations of motion of the OTCL –amplitude and phase variations as a function of the distance between the tip and the surface– to be obtained in order to fit the experimental data. The aim of these equations is to reproduce the observed approach-retract curves and more particularly the increase of the phase delay due to the attractive interaction between the tip and the surface. By using a sphere-plane geometry with an attractive Van der Waals interaction³⁰ describing the interaction between the tip and the surface :

$$V [z (t)] = -\frac{HR}{6 [D - z (t)]}, \quad (1)$$

the equations of motion are given by¹³ :

$$\begin{cases} \cos (\varphi) = Qa(1 - u^2) - \frac{aQ\kappa_a}{3 (d^2 - a^2)^{3/2}} \\ \sin (\varphi) = -ua \end{cases} \quad (2)$$

In equ.1, D is the distance between the sample and the equilibrium position at rest of the OTCL and $z(t) = A \cos (\omega t + \varphi)$ the position of the tip at time t with the driven frequency ω . H and R are the surface Hamaker constant and the tip's apex radius, respectively. From equ.2, one can extract the relationship between the oscillation amplitude and the tip-surface distance :

$$d_{\pm} = \sqrt{a^2 + \left[\frac{Q\kappa_a}{3 \left\{ Q (1 - u^2) \mp \sqrt{1/a^2 - u^2} \right\}} \right]^{2/3}} \quad (3)$$

In equ.3, $a = A/A_0$, $d = D/A_0$ and $u = \omega/\omega_0$ are the reduced amplitude, distance and frequency, respectively. A_0 and ω_0 are the resonance amplitude and resonance frequency of

the OTCL far from the surface, respectively. Q is the quality factor of the OTCL given by $Q = \omega_0/\beta_0$. β_0 is the OTCL damping coefficient in air. $\kappa_a = HR/(k_c A_0^3)$ is a dimensionless parameter which is characteristic of the nonlinear coupling with k_c , the cantilever' stiffness. Thus, varying κ_a with A_0 is equivalent to vary the strength of the attractive interaction¹³.

In order to fit the experimental data, e.g. amplitude and phase variations as a function of the distance between the tip and the surface, it was shown that the introduction of an additional dissipation when the tip does not touch the surface was a necessary requirement that explained the increase of the phase delay^{20,27}. The additional dissipation is modeled as being the consequence of the OTCL energy loss due to the mechanical response of the substrate induced by the attractive interaction with the tip^{20,26,27,28,29}. The substrate is modeled as a viscoelastic, thus described by its local stiffness k_s and damping coefficient γ_s with a relaxation time $\tau_s = \gamma_s/k_s$. These works give a detailed explanation of the origin of an additional damping coefficient β_{int} . Depending on the value of τ_s with regard to the characteristic times of the OTCL –its oscillation period T and the residence time of the tip at the proximity of the surface, τ_{res} – two asymptotic regimes of dissipation can be deduced. τ_{res} is the residence time of the tip in the vicinity of the surface, e.g. when the coupling between the OTCL and the surface is large and is given by $\tau_{res} \simeq \frac{T}{\pi} \sqrt{2\Delta/A}$ ^{20,27}, where $\Delta \simeq D - A$. Depending on the values of τ_s (see fig.1), two asymptotic behaviors are calculated. Results are²⁹ :

$$\text{Short relaxation times } \tau_s \ll \tau_{res} : \beta_{int}(\Delta, A) \simeq \frac{\tau_s K^2}{k_s} \frac{\omega_0^2}{12\sqrt{2}k_c} \times \frac{1}{\Delta^{9/2} A^{3/2}} \quad (4)$$

$$\text{Long relaxation times } \tau_s \gg T : \beta_{int}(\Delta, A) \simeq \frac{K^2}{\gamma_s} \frac{1}{2k_c} \times \frac{1}{\Delta^{7/2} A^{5/2}} \quad (5)$$

with $K = HR/6$. Thus the NC dissipation processes are controlled by the strength of the attractive interaction through a square dependence with the term $(HR)^2$. The limit of short relaxation times is $\tau_s \rightarrow 0$ for which the sample behavior is elastic-like. In that case, the local deformation of the surface follows the action of the oscillating tip without any phase delay (see fig.1). As a consequence, the dissipated energy goes to zero. For long relaxation times, the mechanical susceptibility of the sample scales as $1/\gamma_s$, then also the additional dissipated energy.

The total damping coefficient of the OTCL can be written as an equivalent damping

term^{20,29} :

$$\beta_{eq}(\Delta, A) = \beta_0 + \beta_{int}(\Delta, A), \quad (6)$$

leading to the variations of the sine of the phase (see equ.2) on the form :

$$\sin \varphi = -ua \left(\frac{\beta_{eq}(\Delta, A)}{\beta_0} \right) \quad (7)$$

Equ.7 is the one that is used to fit the experimental phase variations.

The variation of the amplitude without including an additional dissipation is straightforwardly obtained from equ.3. In accordance with the known result that the dissipation reduces the nonlinear effects^{31,32}, a first consequence is a drastic reduction of the size of the hysteresis loop²⁰. When the OTCL approaches the surface, the amplitude variations are similar. The main difference appears at the bifurcation spot where the magnitude of the amplitude jump is slightly frustrated. We have shown that equ.3 was of some help to estimate the value of the HR product²⁰.

III. RESULTS

A. Experimental conditions

Dynamical mode : The silica substrate is cleaned as detailed elsewhere³³ and heated under oxygen flow at 420 °C during 90 minutes in order to remove the water layers and contaminants. Then the sample is put into a glove box under nitrogen controlled atmosphere with one ppm (part per million) of water and oxygen and at room temperature. Experiments of approach-retract curves were performed with a Nanoscope III³⁴ operating in Tapping mode into the glove box. In such conditions, the cantilever behavior is very stable. A commercial silicon tip-cantilever TESP-NCL-W from Nanosensors³⁵ is used, with an announced stiffness of about 40 N.m⁻¹, a measured resonance frequency of 185130 Hz and a quality factor of 500. Particular attention was focussed on the quality of the OTCL whose behavior has to be harmonic for quantitative measurements. Technical remarks concerning the determination of the cantilever parameters and data treatments are detailed in ref.¹³. The experiments were performed at 184944 Hz, corresponding to a phase $\varphi_{free} \simeq -45^\circ$ and an oscillation

amplitude $A_{free} = A_0/\sqrt{2} \simeq 0.707A_0$ for large tip-surface distances. The subscript “free” means that the oscillation conditions are measured at a tip-surface distance for which the tip does not interact with the surface, typically distances of ten nanometers or more.

To investigate the influence of water layers, all the experiments presented in this paper were performed with the same cantilever over three days. Over those three days, no noticeable variation of the OTCL parameters (resonance frequency and quality factor) was observed.

Contact mode : Nanotribological measurements are detailed in a previous paper³⁶. Here, we briefly recall the experimental conditions and present a synthetic result which will then be compared to DFM results (see discussion). The silica substrate is also cleaned and heated at 420 °C under oxygen flow, then exposed to dry conditions. All experiments were performed in a glove box under dry conditions with nitrogen flow. This condition is necessary since experiments performed in air (under uncontrolled humidity rate) were not as much reproducible to extract a significant variation of the adhesion and friction as a function of the temperature. Force curves and friction loops were recorded at temperature varying between 25 °C and 170 °C³⁶.

B. Results obtained in Tapping mode

1. Noncontact situations : evaluation of the HR product

When the sample is taken out of the furnace, corresponding to the reference time – set time zero –, approach-retract curves are recorded every two or three hours, three days long. During the approach-retract curve, when the bistable behavior occurs, the tip is at a vertical location far enough from the surface, in the range of one nanometer or more, to reduce the contribution of the NC dissipation. As a consequence, one can estimate that the bifurcation is only controlled by HR/k_c and A_0 through the κ_a dependence. Nevertheless, note that the strength of the attractive force scaling as $\sqrt{1/A}^9$ (see also the A dependence in τ_{res}), a too low value of the amplitude can not be used to perform the fits. Therefore, the curves for which the noncontact (NC) situations occur allow to get an evaluation of the HR/k_c product from equ.3. For this set of experiments, the amplitude at which the first NC situation happens is $A_{free} = 19$ nm ($A_0 = 27$ nm). To simplify the analysis and use the

fit of the experimental NC curves, a typical value of the amplitude used is $A_{free} = 12.5$ nm ($A_0 = 18$ nm). The experimental measurements are then compared at different times.

In fig.2 are reported comparisons between experimental and theoretical curves for different amplitudes and different times. The equ.3 used to fit the experimental data gives a reasonable agreement. The average value of the coefficient HR/k_c extracted from the fits is $0.46 \cdot 10^{-27}$ m³. Thus, by taking $k_c \simeq 40$ N.m⁻¹, we get $HR \simeq 18 \cdot 10^{-27}$ J.m. Taking into account the fact that the very first NC situation is obtained for $A_{free} = 19$ nm, it's expected that the radius of the tip is not very small since we usually observe NC situations on the silica for $A_{free} \simeq 10$ nm, or less¹³. Thus in that case, let's consider $R \simeq 20$ nm. As a consequence, we get for the silica $H \simeq 10^{-19}$ J. This evaluation is in agreement with a previous result (see below).

The fits do not provide an accurate quantitative value of HR but allow to evaluate the variation of the strength of the attractive interaction between the tip and the surface as a function of time. The result of the fits obtained at different times for $A_{free} = 12.5$ nm are given in fig.3. Any variation of the value of HR/k_c is noticed three days long. Since the radius of the tip and the cantilever stiffness are constant parameters, a constant value of HR/k_c means that the Hamaker constant remains nearly the same. Therefore, whatever the evolution of the silica surface during those three days, this evolution does not lead to a noticeable variation of the attractive interaction between the tip and the surface.

The same method was used to compare the attractive interaction between a tip and a silica surface and the same tip and a grafted silica surface. From the fits, it was deduced that $(HR)_{silica} \simeq 5 \cdot 10^{-27}$ J.m and $(HR)_{grafted\ silica} \simeq 11.5 \cdot 10^{-27}$ J.m²⁰. While it is difficult to evaluate the error on the H values, the use of equ.3 appears quite helpful either to compare two different surfaces or to evaluate the relative evolution of the surface properties for a given tip.

2. Intermittent contact situations : evolution of the phase delay

As detailed in refs.^{20,29}, in Tapping mode it is more convenient to use intermittent contact (IC) situations to evaluate the contribution of the NC dissipation on the phase delay. The main reason is that one needs to use an average distance between the tip and the surface, Δ , that gives an order of magnitude of the strength of the attractive interaction

$HR/[6(D-z(t))^2] \simeq HR/(6\Delta^2)$. To simplify our evaluation, we consider a fixed value of Δ , typically $\Delta = \bar{\Delta} = 0.5$ nm. These assumptions are easily achieved with a large oscillation amplitude. Note that for IC situations, $\Delta = D - A$ is less than the percent of the amplitude and therefore $\bar{\Delta} \ll A$. Thus, while for pure NC situations one has two varying parameters, the closest distance Δ and the oscillation amplitude A , for IC situations a fixed value of the closest distance $\bar{\Delta}$ appears as a reasonable working assumption to evaluate the average contribution of the attractive interaction.

Experimental phase variations at different times and the theoretical curves obtained from equ.7 with the large values of τ_s ($\beta_{int} \propto A^{-5/2}$, equ.5) are shown in fig.4. The phase jump increases as a function of time. This is predicted to be the consequence of an increase of the NC dissipation²⁰ (see also discussion). The phase variations are fitted as a function of the observed variations of the oscillation amplitude. There is only one varying parameter which is $1/\gamma_s$, the others parameters being evaluated (HR), or estimated ($k_c, \bar{\Delta}$). All the theoretical curves are obtained with the power law $A^{-5/2}$. Fits performed with the other asymptotic regime, short relaxation times, with a power law $A^{-3/2}$ (equ.4) can be separated unambiguously, as shown with fig.5.

IV. DISCUSSION

The mechanical susceptibility $1/\gamma_s$ extracted from the fits exhibits a marked evolution versus time (fig.6). Since the fits of the HR product lead to a constant value (fig.3), this result indicates a decrease of the surface damping coefficient. It is noteworthy recalling that the amount of NC dissipated energy corresponds to the ability of the surface to exhibit a viscoelastic displacement induced by the attractive interaction. Therefore for surface relaxation times larger than that of the oscillation period, when γ_s decreases, a surface displacement proportional to $1/\gamma_s$ leads to an increase of the NC dissipated energy. This is what is straightforwardly observed with the increase of the phase jumps of the curves with time (fig.4).

Such a variation of γ_s indicates an evolution of the surface structure and properties as a function of time. Just after the heating process, only a few water molecules, if any, cover the surface and are tightly bounded to the silica. In that case, the water layer might be considered as an amorphous layer with long relaxation times corresponding to a high

damping coefficient. The mechanical susceptibility of these molecules is weak so that the surface is weakly perturbed by the tip-surface attractive interaction. When the sample is exposed, even in a dry atmosphere, water molecules are more and more adsorbed on the surface, leading to a more fluid-like behavior of the surface with a higher molecular mobility and, in turn, a shorter relaxation time. Nevertheless, as shown with fig.5, the use of the short relaxation times model doesn't provide a good agreement with the observed phase variations. Even 90 hours after the beginning of the experiments, it's still possible to fit the experimental data with the long time model (fig.4, diamonds symbols). In ref.²⁰, the experimental phase variations on the silica could not be fitted with the long times model, but only with the short times one. But in that case, no thermal treatment of the silica had been used and the surface was placed into the glove box for many days. From these results, one can deduce that the quantity of water layers on this latter surface should be larger than the one on the thermally treated surface, even 90 hours after the beginning of the experiments.

While equs.4 or 5 aim at describing pure NC situations, questions rise about the origin of the information which is measured within Tapping experiments. As explained above, in Tapping mode, one has two varying parameters to fit the experimental variations : A and Δ . A varying during the approach-retract curves, Δ too. This leads to complex situations if one wants to extract NC dissipation parameters from the pure NC situations. This is mainly the reason why, IC situations are used, Δ being fixed to an average value, $\bar{\Delta}$, of about a few angstroms. But as a consequence, $\bar{\Delta}$ might be as well fixed to the so-called contact distance³⁰, $d_c \simeq 0.165$ nm, thus changing the magnitude of γ_s . For instance, by choosing $\bar{\Delta} = 0.25$ nm instead of $\bar{\Delta} = 0.5$ nm, the value of γ_s obtained would be 11 times larger because of the $\bar{\Delta}^{-7/2}$ dependence in equ.5. This makes absolute quantitative measurements difficult to achieve. As a consequence, the magnitude of γ_s reported in fig.6 is only indicative since it could has been one order of magnitude larger.

The DFM results are in excellent agreement with those obtained from Contact mode and FTIR spectroscopy³⁶. In these experiments, we had focused on the influence of capillary effects due to the presence of water layers on the nanotribological properties as a function of the sample temperature. The variations of the pull off force and of the frictions forces were reasonably well explained by assuming the creation of a water meniscus between the tip

and the surface. When the tip is pulled off the surface (adhesion force) or moved laterally (tangential force or friction), a gap is created between the tip and the silica surface and is filled with a liquid phase. The AFM measurements show a net decrease of the measured forces as the temperature increases. As an example, the decrease of the pull off force as a function of the temperature is shown in fig.7. The abrupt decrease observed around 100°C suggests that capillary forces provide a major contribution to the pull off and tangential forces at room temperature.

The nature of the water layer on silica versus temperature was also analyzed by FTIR spectroscopy and correlated to the water layers morphology. A qualitative analysis of the spectrums obtained gives two kinds of water layers : liquid layers, which are removed above 100°C and strongly adsorbed water molecules with a solid-like behavior that still remain at 150°C and under vacuum. In this latter case, the water layers become more structured due to the proximity of the substrate. For the liquid structure, we assume a molecular mobility that is weakly dependent on the thickness of the water film. When the temperature increases, the decrease of these forces is related to a structural modification of the water layers.

The comparison between the evolution of the damping coefficient as a function of time deduced from the Tapping experiments (fig.6) and the one of the normalized pull off force (fig.7) as a function of the temperature, suggests that the first Tapping measurement performed at time zero corresponds to the data measured at 120°C with the Contact mode (arrow 1 on both figures). Thus we can deduce an equivalence between time exposure of the sample to dry conditions and temperature of the sample. The covering of the silica going on with time, e.g. the quantity of the water molecules adsorbed on the surface increasing, the damping coefficient decrease can be interpreted as a decrease of the equivalent temperature of the sample (from arrow 1 to 2 on fig.6 and from 2 to 1 on fig.7).

Acknowledgements

The authors thank the Région Aquitaine for financial support.

V. CONCLUSION

Dynamic Force Microscopy experiments were performed to investigate the growth of water layers on a silica surface exposed to a rather dry atmosphere as a function of time.

Noncontact dissipation due to the attractive interaction between the tip and the surface is included in the theoretical developments. This allows to describe the evolution of the OTCL phase as a function of time that corresponds to changes of the water layers structure. The equations obtained from the model are able to reproduce with a good agreement the experimental observations. These variations can only be reproduced from the model taking into account rather long relaxation times. The damping coefficient deduced shows a marked decrease as a function of time. As a consequence, the evolution of the mechanical susceptibility of the silica surface indicates the contamination of the surface with water molecules as a function of time.

These DFM observations are in good agreement with previous tribological and infra-red measurements for which the contamination of a silica surface with water molecules was investigated as a function of the sample temperature.

References

- ¹ Leclère, P., Lazzaroni, R., Brédas, J.-L., Yu, J.M., Dubois, P., Jérôme, R. *Langmuir* **12**(18), 4317–4320 (1996).
- ² Magonov, S.N., Elings, V., Denley, D., Wangbo, M.H. *Surf. Sci.* **389**, 201–211 (1997).
- ³ Rivetti, C., Guthold, M., Bustamante, C. *J. Mol. Biol.* **264**, 919–932 (1996).
- ⁴ Shlyakhtenko, L.S., Gall, A.A., Weimer, J.J., Hawn, D.D., Lyubchenko, Y.L. *Biophys. J.* **77**, 568–576 (1999).
- ⁵ Barrat, A., Silberzan, P., Bourdieu, L., Chatenay, D. *Europhys. Lett.* **20**(7), 633–638 (1992).
- ⁶ Vallant, T., Brunner, H., Mayer, U., Hoffmann, H., Leitner, T., Resch, R., Friedbacher, G. *J. Phys. Chem. B* **102**, 7190–7197 (1998).
- ⁷ Tamayo, J., Garcia, R. *Appl. Phys. Lett.* **71**(16), 2394–2396 (1997).
- ⁸ Haugstad, G.D., Hammerschmidt, J.A., Gladfelter, W.L. *Microstructures and Tribology of Polymer Surfaces*. ACS Boston, (1998).
- ⁹ Aimé, J.-P., Michel, D., Boisgard, R., Nony, L. *Phys. Rev. B* **59**(3), 2407–2416 (1999).
- ¹⁰ Marsaudon, S., Leclère, Ph., Dubourg, F., Lazzaroni, R., Aimé, J.-P. *Langmuir* **16**, 8432–8437 (2000).
- ¹¹ Dubourg, F., Aimé, J.-P. *Surf. Sci.* **466**, 137–143 (2000).
- ¹² Garcia, R., San Paulo, A. *Phys. Rev. B* **60**(7), 4961–4967 (1999).
- ¹³ Nony, L., Boisgard, R., Aimé, J.-P. *J. Chem. Phys.* **111**(4), 1615–1627 (1999).
- ¹⁴ Nony, L., Boisgard, R., Aimé, J.-P. *Biomacromolecules* **2**, 827–835 (2001).
- ¹⁵ Tamayo, J., Garcia, R. *Appl. Phys. Lett.* **73**(20), 2926–2928 (1998).
- ¹⁶ Gotsmann, B., Seidel, C., Anczykowski, B., Fuchs, H. *Phys. Rev. B* **60**(15), 11051–11061 (1999).
- ¹⁷ Gauthier, M. et Tsukada, M. *Phys. Rev. B* **60**(16), 11716–11722 (1999).
- ¹⁸ Dorofeyev, I., Fuchs, H., Wenning, G., Gotsmann, B. *Phys. Rev. Lett.* **83**(12), 2402–2405 (1999).
- ¹⁹ Bennewitz, R., Foster, A.S., Kantorovich, L.N., Bammerlin, M., Loppacher, Ch., Schär, S., Guggisberg, M., Meyer, E., Shluger, A.L. *Phys. Rev. B* **62**(3), 2074–2084 (2000).
- ²⁰ Aimé, J.-P., Boisgard, R., Nony, L., Couturier, G. *J. Chem. Phys.* **114**(11), 4945–4954 (2001).
- ²¹ Binggeli, M., Mate, C.M. *J. Vac. Sci. Technol. B* **13**(3), 1312–1315 (1995).

- ²² Weisenhorn, A.L., Hansma, P.K., Albrecht, T.R., Quate, C.F. *Appl. Phys. Lett.* **54**(26), 2651–2653 (1989).
- ²³ Scherge, M., Li, X., Schaefer, J.A. *Mat. Res. Soc. Symp. Proc.* **522**, 481–486 (1998).
- ²⁴ De Pablo, P.J., Colchero, J., Luna, M. et al. *Phys. Rev. B* **61**(29), 14179–14183 (2000).
- ²⁵ Luna, M., Colchero, J., Gil, A. et al. *Appl. Surf. Sci.* **157**, 393–397 (2000).
- ²⁶ Couturier, G., Aimé, J.-P., Salardenne, J., Boisgard, R. *Eur. Phys. J. AP* **15**, 141–147 (2001).
- ²⁷ Couturier, G., Aimé, J.-P., Salardenne, J., Boisgard, R. *J. Phys. D : Appl. Phys.* **34**, 1266–1270 (2001).
- ²⁸ Couturier, G., Aimé, J.-P., Salardenne, J., Boisgard, R., Gourdon, A., Gauthier, S. *Appl. Phys. A (Material Science and Processing)* **72**, s47–s50 (2001).
- ²⁹ Boisgard, R., Aimé, J.-P., Couturier, G. Accepted in *Appl. Surf. Sci.*
- ³⁰ Israelachvili, J.N. *Intermolecular and Surface Forces*. Academic Press, New York, 2nd edition, (1992).
- ³¹ Thompson, J.J. , Stewart, H.B. *Non Linear Dynamics and Chaos*. J. Wiley and sons, New York, (1991).
- ³² Aimé, J.-P., Boisgard, R., Nony, L., Couturier, G. *Phys. Rev. Lett.* **82**(17), 3388–3391 (1999).
- ³³ Gauthier, S., Aimé, J.-P., Bouhacina, T., Attias, A.-J., Desbat, B. *Langmuir* **12**, 5126–5137 (1996).
- ³⁴ Digital Instruments, Veeco Metrology Group, Santa Barabara CA (USA).
- ³⁵ Nanosensors, Veeco Instruments SNC, France.
- ³⁶ Bouhacina, T., Desbat, B., Aimé, J.-P. *Tribology Let.* **9**(1,2), 111–117 (2000).

Figures

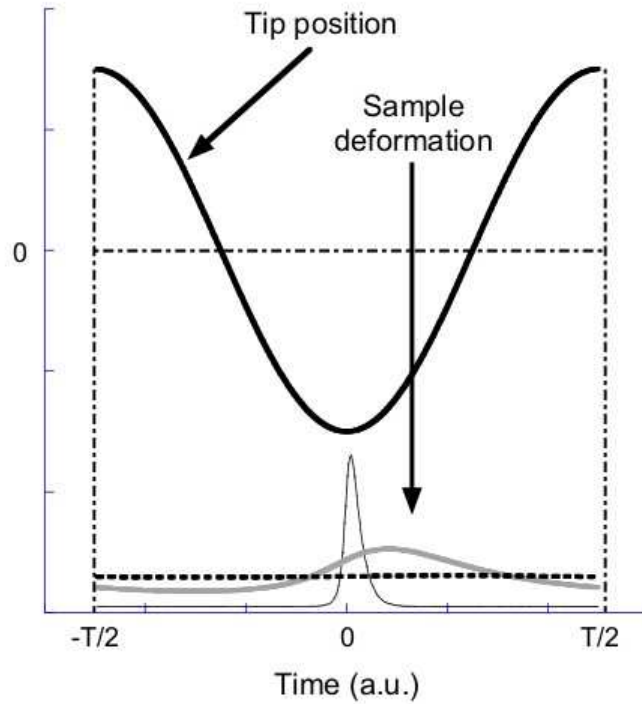


FIG. 1: Sketch of the action of the oscillating tip on the sample. The viscoelastic behavior of the surface (γ_s, k_s) implying that it can be deformed under the action of the tip-surface attractive force. Depending on the value of its relaxation time $\tau_s = \gamma_s/k_s$ with regard to the period T and the residence time τ_{res} (long, $\tau_s \gg T$: thick black dashed line, short, $\tau_s \ll \tau_{res}$: thin black line or intermediary : thick grey line), various expressions of the additional dissipation β_{int} can be obtained (see text).

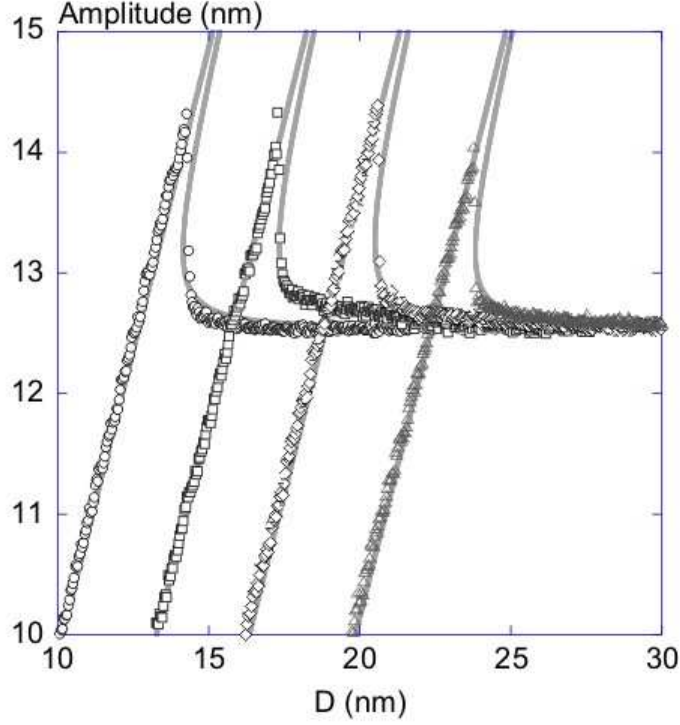


FIG. 2: Experimental noncontact amplitude variations (open black symbols) versus tip-surface distance for $A_{free} = 12.5$ nm ($A_0 = 18$ nm) as a function of time and their comparisons with theoretical curves deduced from equ.3 (continuous grey lines). The theoretical curves are calculated in order to fit the location of the bifurcation, thus giving an evaluation of HR/k_c . The general experimental parameters are given in the text. Circles, $time = 0.7$ hours; squares, $time = 7$ hours; diamonds, $time = 30$ hours; triangles, $time = 76$ hours. The horizontal locations of the curves have been arbitrarily shifted in order to show all the variations.

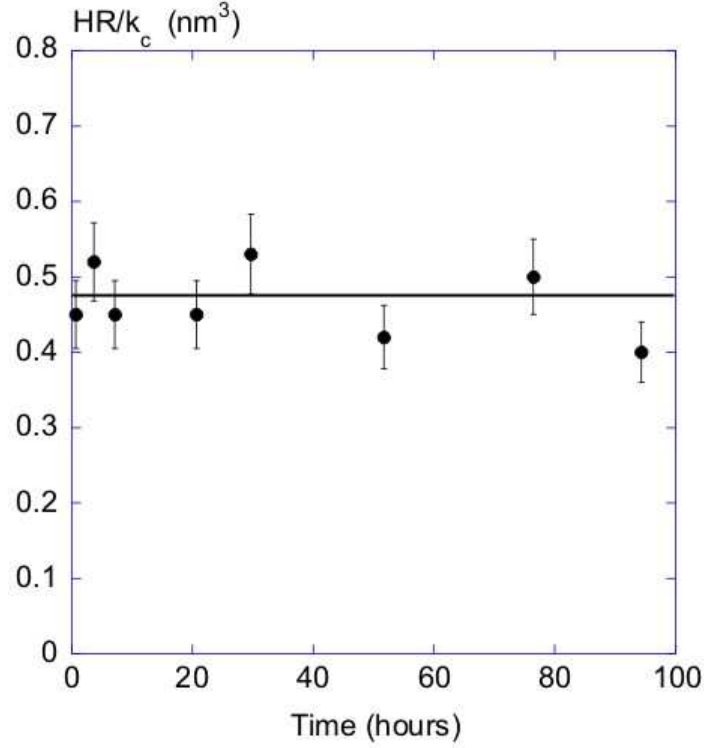


FIG. 3: Values of HR/k_c deduced from the fits of the experimental amplitudes variations as a function of time. The fits were performed on the curves obtained for $A_{free} = 12.5$ nm (see fig.2). HR/k_c doesn't evolve with time and the average value is $0.46 \cdot 10^{-27}$ m³. Since R and k_c are constant parameters, a constant value of HR/k_c means that the Hamaker constant remains nearly the same, $H \simeq 10^{-19}$ J (see text).

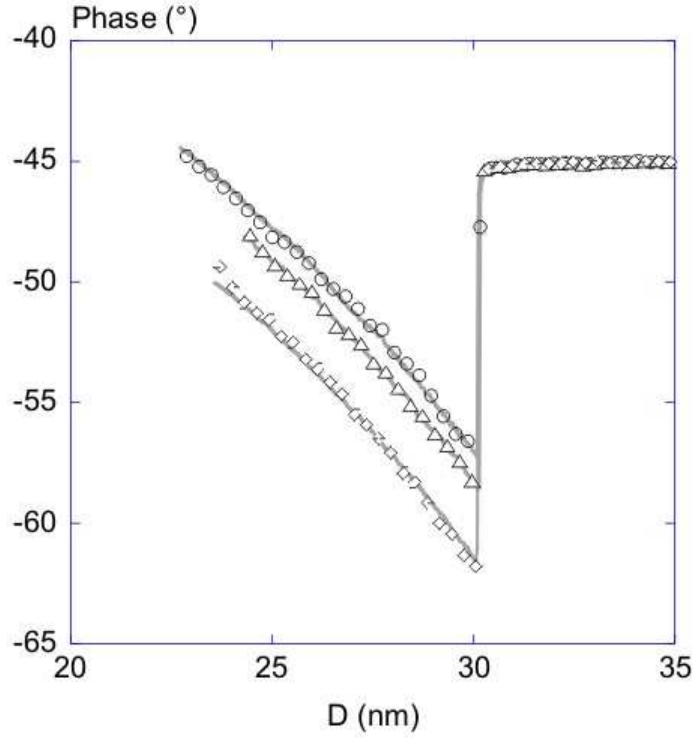


FIG. 4: Experimental intermittent contact phase variations (open black symbols) versus tip-surface distance as a function of time and their comparisons with theoretical curves (continuous grey lines) deduced from equ.7. The curves were obtained with $A_{free} = 36$ nm ($A_0 = 51$ nm). The other parameters are : circles, $time = 7$ hours; triangles, $time = 21$ hours; diamonds, $time = 90$ hours. The increase of the phase jump as a function of time is characteristic of an increase of the dissipated energy.

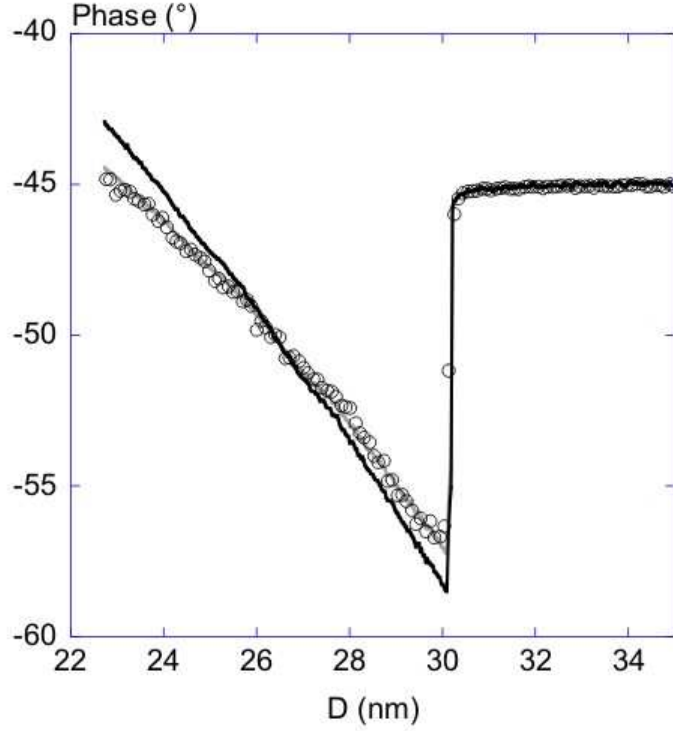


FIG. 5: Experimental phase variation (open black circles) versus tip-surface distance and its comparison with theoretical curves deduced from the long relaxation times model, $A^{-5/2}$ equ.5 (continuous grey line) and the short relaxation times model, $A^{-3/2}$ equ.4 (continuous black line). The experimental parameters are $A_{free} = 36$ nm ($A_0 = 51$ nm) and $time = 7$ hours.

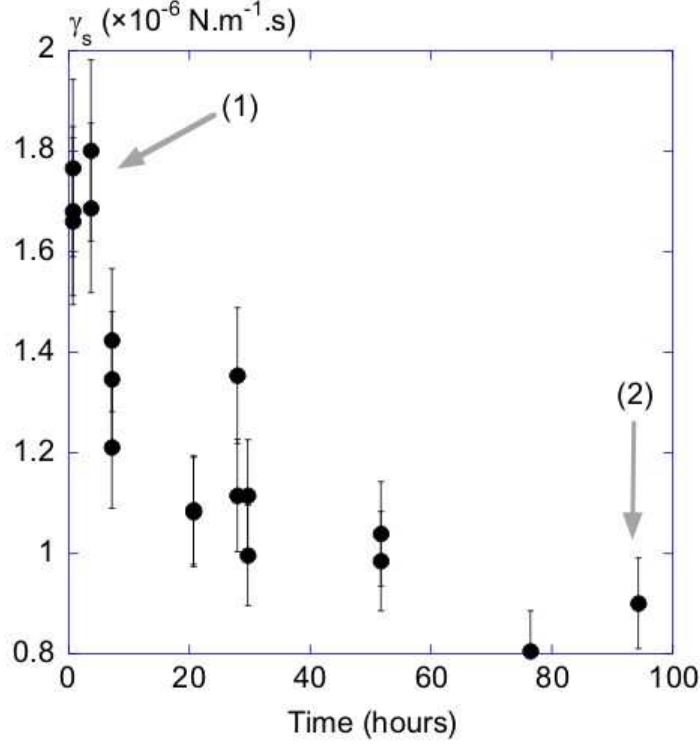


FIG. 6: Evolution of the γ_s parameter with time deduced from the fits of the experimental phase variations with the long relaxation times model. The values of γ_s depend on the evaluation of HR and $\bar{\Delta}$ (see text). The net decrease observed, corresponding to an increase of the NC dissipation, is the consequence of the increase of the quantity of water molecules adsorbed on the silica surface with time. The arrows 1 and 2 indicate the time-temperature equivalence that can be extracted by comparing the Tapping mode and Contact mode experiments (see text). For instance, arrow 1 indicates a structure of the water layer corresponding to a temperature above 100°C , whereas arrow 2 corresponds to a structure of the water layers observed at room temperature (see fig.7).

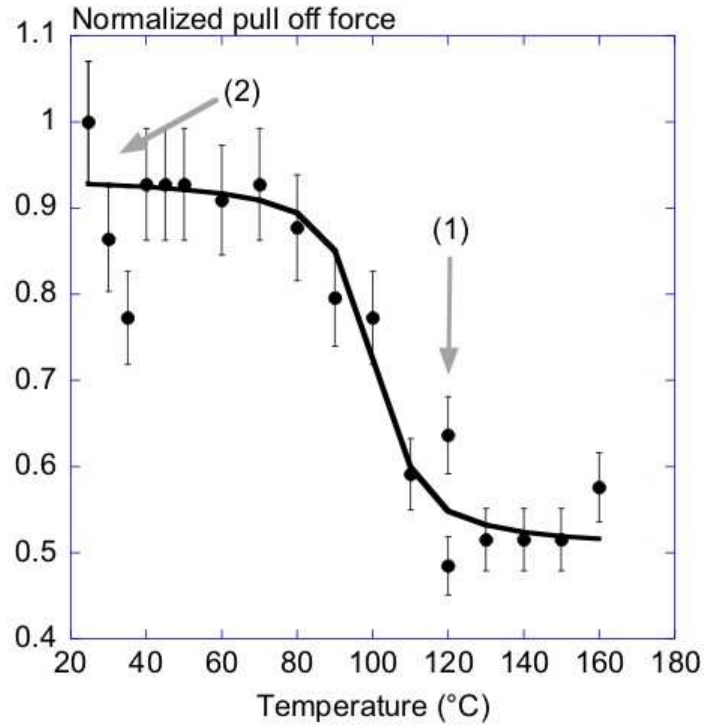


FIG. 7: Evolution of the normalized pull off force as a function of the silica sample temperature deduced from Contact mode experiments³⁶. The normalization pull off force is 82 nN. The black line is a guide line for eyes. The arrows 1 and 2 indicate the time-temperature equivalence that can be extracted by comparing the Tapping mode and Contact mode experiments (see text and fig.6).